SUPPORTING INFORMATION

Hafnium vs Zirconium, The Perpetual Battle for Supremacy in Catalytic Olefin Polymerization: A Simple Matter of Electrophilicity?

Antonio Vittoria,[1] Georgy P. Goryunov,[2] Vyatcheslav V. Izmer,[2] Dmitry S. Kononovich,[2] Oleg V. Samsonov,[2] Francesco Zaccaria,[3] Gaia Urciuoli,[1] Peter H. M. Budzelaar,[1] Vincenzo Busico,[1] Alexander Z. Voskoboynikov,[2] Dmitry V. Uborsky,[2] Christian Ehm[1*] and Roberta Cipullo[1*]*

[1] Dipartimento di Scienze Chimiche, Università di Napoli Federico II, Via Cintia, 80126 Napoli, Italy;

[2] Department of Chemistry, Lomonosov Moscow State University, 1/3 Leninskie Gory, 119991 Moscow, Russia;

[3] Dipartimento di Chimica, Biologia e Biotecnologie and CIRCC, Università di Perugia, 06123 Perugia, Italy

[*] Correspondence: duborsky@med.chem.msu.ru (D.V.U.); christian.ehm@unina.it (C.E.); rcipullo@unina.it (R.C.)

Contents

1. Synthesis of complexes

1.1 General Details

All manipulations with compounds, which are sensitive to moisture and air, were performed either in an atmosphere of argon using a standard Schlenk technique or in an inert atmosphere (Ar) of glove box (MBraun). ^{1}H, ^{13}C and ^{19}F spectra were recorded on Bruker Avance-400 spectrometer for 1–10% solutions in deuterated solvents. Chemical shifts for ^{1}H and ^{13}C are reported relatively to TMS and referenced to the residual ^{1}H or ^{13}C resonances of the deuterated solvents. C, H microanalyses were done using a «Elementar Vario MICRO cube» analyzer.

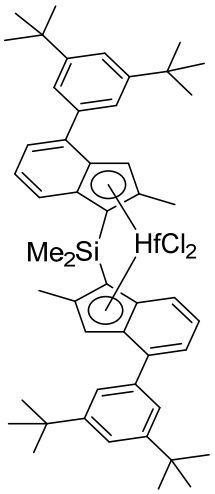

Synthesis of Hf-1. To a solution of 5.20 g (7.5 mmol) of bis[4-(3,5-di-*tert*-butylphenyl)-2-methyl-1*H*-inden-1-yl](dimethyl)silane in 250 mL of ether, 6.0 mL *n*BuLi (2.5 M in hexane, 15.0 mmol) was added at 0 °C. The mixture was stirred for 12 h at room temperature, cooled to -80 °C, and 2.40 g of $HfCl_4$ (7.5 mmol) was added. After that, the ether was evaporated, and the residue was taken up in hot toluene (100 mL), and filtered (G4), the filter cake was washed with additional 2×20 mL of hot toluene. The filtrate was evaporated to ~50 mL volume, and 30 mL of n-hexane was added. The precipitated solid was filtered and dried in vacuum. This gave 0.19 g (3%) of **Hf-1**. Anal. Calcd for $C_{50}H_{62}Cl_2HfSi$: C, 63.85; H, 6.64. Found: C, 64.03; H, 6.75. ^{1}H NMR (400 MHz C_6D_6) δ 7.70 (d, J = 8.7 Hz, 2H), 7.53 (d, J = 1.7 Hz, 4H), 7.41 (m, 2H), 7.40 (d, J = 7.0 Hz, 4H), 7.09 (dd, J = 8.7, 7.0 Hz, 2H), 6.90 (s, 2 H), 2.36 (s, 6H), 1.34 (s, 6H), 1.32 (s, 36H). $^{13}C\{^{1}H\}$ NMR (100 MHz, $CDCl_3$): δ 150.6, 139.0, 138.2, 132.6, 131.4, 125.8, 125.7, 125.2, 123.6, 123.0, 121.1, 120.8, 83.9, 34.7, 31.1, 18.1, 2.2.

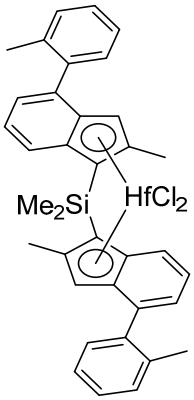

Synthesis of Hf-2. To a solution of 6.34 g (12.8 mmol) of bis[4-(2-methylphenyl)-2-methyl-1*H*-inden-1-yl](dimethyl)silane in 250 mL of ether, 10.2 mL *n*BuLi (2.5 M in hexane, 25.5 mmol) was added at 0 °C. The mixture was stirred for 2 h at room temperature, cooled to -80 °C, and 4.09 g $HfCl_4$ (12.8 mmol) was added. The mixture was then stirred overnight at room temperature. The obtained suspension was filtered while hot through a pad of Celite; the filter cake was washed with additional 2×20 mL of hot toluene. The filtrate was evaporated to ~40 mL volume, and 40 mL of n-hexane was added. The precipitated solid was filtered and dried in vacuum. This gave 0.64 g (6%) of **Hf-2** containing 0.5 equivs of cocrystallized toluene. Anal. Calcd for $C_{36}H_{34}Cl_2HfSi{\cdot}0.5C_7H_8$: C, 60.04; H, 4.85. Found: C, 59.41; H, 4.72. ^{1}H NMR (400 MHz, $CDCl_3$) δ 7.68 (d, J = 8.7 Hz, 2H), 7.53 (br. s., 2H), 7.28–7.21 (br. s., 6H), 7.14–7.20 (m, 2H), 7.05 (dd, J = 8.7, 6.9 Hz, 2H), 6.43 (br. s., 2H), 2.33 (m, 6H), 2.06 (br. s., 6H), 1.32 (s, 6H). $^{13}C\{^{1}H\}$ NMR (101 MHz, C_6D_6): δ 139.9, 138.0, 135.9, 134.4, 133.1, 130.6, 130.5, 129.7, 128.9, 126.9, 125.9, 125.8, 124.7, 121.2, 84.9, 20.5, 18.8, 2.5.

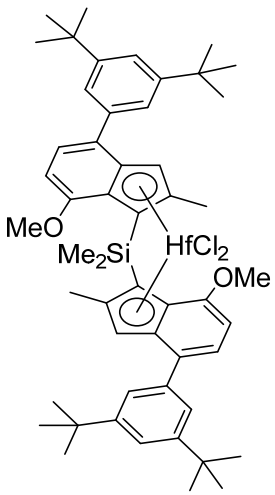

Synthesis of Hf-3. To a solution of 10.21 g (13.56 mmol) of bis[4-(3,5-di-*tert*-butylphenyl)-7-methoxy-2-methyl-1*H*-inden-1-yl](dimethyl)silane in 200 mL of ether, 11.2 mL (27.22 mmol) of 2.43 M *n*BuLi in hexanes was added in one portion at -50 °. The mixture was stirred for 4 h at room temperature, then cooled to -50 °C and 4.35 g (13.58 mmol) of $HfCl_4$ was added. The mixture was stirred for 48 h at room temperature and then evaporated almost to dryness. The residue was taken up in 350 mL of hot toluene. The obtained mixture was filtered while hot through glass frit (G4) and the filtrate was evaporated to ~250 mL volume. A yellow crystalline solid precipitated from this solution after standing overnight at room temperature was collected and dried in vacuum. This gave 7.19 g of *meso*-**Hf-3** containing cocrystallized toluene, which was equal to 6.51 g (48%) of pure *meso*-**Hf-3**. The mother liquor was evaporated to ~50 mL volume. A yellow crystalline solid precipitated from this solution after standing overnight at room temperature was collected and dried in vacuum. This gave an additional 1.3 g of *meso*-**Hf-3** containing cocrystallized toluene, which was equal to 1.18 g (9%) of pure *meso*-**Hf-3**. The mother liquor was evaporated to a highly viscous oil, which was triturated with 40 mL of n-hexane. Yellow precipitate formed was filtered off and dried in vacuum. This procedure gave 1.40 g (10%) of a ~1/1 mixture of **Hf-3** (racemate) and *meso*- **Hf-3**. The total yield of **Hf-3** and *meso*-**Hf-3** was 67%. *meso*-**Hf-3**, ^{1}H NMR (400 MHz, $CDCl_3$): *δ* 7.46 (d, *J* = 1.7 Hz, 4H), 7.37 (t, *J* = 1.7 Hz, 2H), 7.10 (d, *J* = 7.8 Hz, 2H), 6.82 (s, 2H), 6.20 (d, *J* = 7.8 Hz, 2H), 3.88 (s, 6H), 2.61 (s, 6H), 1.34 (s, 36H), 1.32 (s, 3H), 1.25 (s, 3H).

Isomerization of meso-**Hf-3** *to* **Hf-3.** To a mixture of 7.19 g (6.51 g excluding cocrystallized toluene, 6.51 mmol) of *meso*-**Hf-3** and 600 mg (14.2 mmol) of LiCl 150 mL of THF was added. This mixture was stirred for 48 h at 64 °C. That resulted in almost quantitative isomerization of *meso*-**Hf-3** to racemic **Hf-3**. The mixture was evaporated to dryness, the solid residue was taken up in 400 mL of hot toluene. The obtained suspension was filtered while hot through glass frit (G4) and the filtrate was evaporated to ~50 mL volume. A yellow crystalline solid precipitated from this solution after standing overnight at room temperature was collected and dried in vacuum. This gave 5.12 g of **Hf-3**. The mother liquor was evaporated almost to dryness and the residue was triturated with 40 mL of n-hexane. A yellow precipitate thus formed was filtered off and dried in vacuum. This gave an additional 1.07 g of **Hf-3**. Thus, the total yield of **Hf-3** from *meso*-**Hf-3** was 6.19 g (95%). The analytical data matched that from the literature.[1]

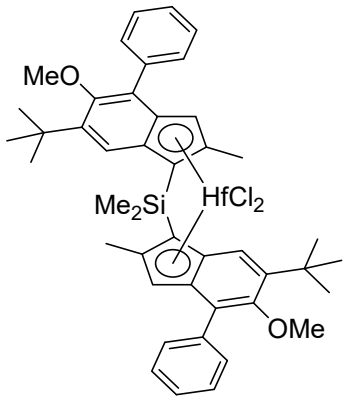

Synthesis of Hf-4. To a suspension of 11.6 g (18.1 mmol) of bis(6-*tert*-butyl-5-methoxy-2-methyl-4-phenyl-1*H*-inden-1-yl)(dimethyl)silane in 150 mL of Et_2O, 14.9 mL (36.2 mmol) of 2.43 M *n*BuLi in hexanes was added in one portion at -50 °C. The mixture was stirred overnight at room temperature, then cooled to -50 °C and 5.8 g (18.1 mmol) of $HfCl_4$ was added. The mixture was stirred for 24 h at room temperature and then evaporated to dryness. The residue was taken up in 150 mL of hot toluene and the mixture was filtered while hot through glass frit (G4). The filtrate was evaporated to ~50 mL volume. A yellow solid precipitated after standing overnight at room

temperature was filtered and dried in vacuum. This gave 3.3 g (21%) of **Hf-4**. The mother liquor was evaporated to ~30 mL volume. A yellow solid precipitated after standing overnight at room temperature was filtered and dried in vacuum. This gave an additional 6.4 g (40%) of **Hf-4**. The mother liquor was evaporated to an oil which was triturated with 20 mL of n-hexane. A precipitated yellow solid was filtered and dried in vacuum to give an additional 2.38 g (15%) of **Hf-4**. The total yield **Hf-4** was 12.08 g (75%). **Hf-4**: Anal. calc. for $C_{44}H_{50}Cl_2HfO_2Si$: C, 59.49; H, 5.67. Found: C, 59.84; H, 5.81. ^{1}H NMR (400 MHz, $CDCl_3$): *δ* 7.61 (very br.s, 4H), 7.56 (s, 2H), 7.43 (dd, *J* = 7.4 Hz, 4H), 7.32 (t, *J* = 7.4 Hz, 2H), 6.50 (s, 2H), 3.39 (s, 6H), 2.25 (s, 6H), 1.39 (s, 18H), 1.28 (s, 6H). ^{13}C{^{1}H} NMR (101 MHz, $CDCl_3$): *δ* 159.8, 143.8, 137.0, 133.1, 132.5, 129.7, 128.5, 127.2, 126.5, 121.3, 121.1, 119.1, 82.9, 62.7, 35.7, 30.4, 18.2, 2.4.

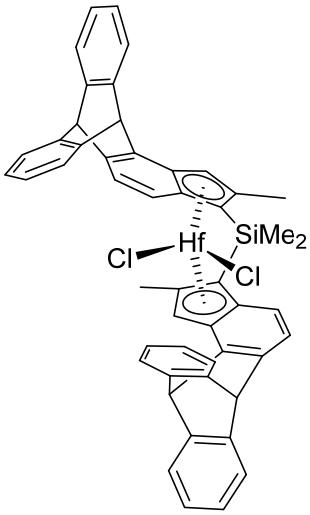

Synthesis of Hf-5-Cl$_2$. To a solution of 1.55 g (2.32 mmol) of bis(2-methyl-*1H*-cyclopenta[a]triptycene-1-yl)(dimethyl)silane in 50 ml of diethyl ether, 1.85 ml (4.63 mmol) of 2.5 M *n*BuLi in hexanes was added at room temperature. This mixture was stirred overnight, and then 1.08 g (2.32 mmol) of $HfCl_4(THF)_2$ was added in one portion at -80 °C. The resulting mixture was stirred for 24 h at room temperature and then evaporated to dryness. Further on, 50 ml of toluene was added. The resulting mixture was heated to 110 °C and filtered through the short pad of Celite 503. The filtrate was evaporated to dryness. The residue was recrystallized from toluene giving 610 mg (28%) of mixture of *rac*- **Hf-5-Cl$_2$** and *meso*- **Hf-5-Cl$_2$** (7:1 molar ratio) as yellow crystals. *Rac*-isomer: ^{1}H NMR (400 MHz, $CDCl_3$): δ (ppm) 7.20-7.41 (m, 14H), 6.90-7.03 (m, 6H), 6.72 (s, 2H), 5.49 (s, 2H), 5.48 (s, 2H), 2.23 (s, 6H), 1.16 (s, 6H). ^{13}C{^{1}H} NMR (100 MHz, $CDCl_3$): *δ* 146.30, 146.2, 145.2, 143.6, 141.1, 133.5, 130.8, 129.0, 128.2, 125.3, 124.75, 124.73, 124.65, 124.5, 123.9, 123.36, 123.31, 122.7, 122.6, 121.7, 115.5, 84.3, 54.4, 51.4, 18.6, 2.5.

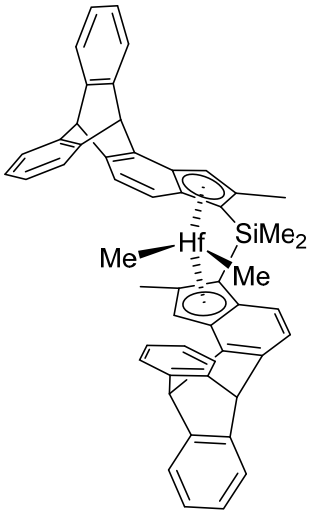

Synthesis of Hf-5. To a suspension of 500 mg (0.545 mmol) of the of *rac*-**Hf-5-Cl$_2$** and *meso*-**Hf-5-Cl$_2$** (7:1 molar ratio) in 40 ml of toluene 570 ul of 2.9 M MeMgBr (1.64 mmol) in ether was added at room temperature. This mixture was stirred for 24 h at 100 °C and then evaporated to dryness in vacuum. To the residue 40 ml of toluene were added and the mixture was heated up to 110 °C and then was passed while hot through a short pad of Celite 503. The filtrate was evaporated to dryness. According to ^{1}H NMR analysis a pure mixture of dimethyl complexes **Hf-5** (racemate) and *meso*-**Hf-5** (molar ratio 7:1) was obtained. The residue was recrystallized from toluene/hexane mixture giving 190 mg (37%) of pure racemic **Hf-5** containing 0.5 equivs of cocrystallized toluene. ^{1}H NMR (400 MHz, $CDCl_3$): δ (ppm) 7.31-7.35 (m, 6H), 7.27 (d, *J* = 7.0 Hz, 2H), 7.22 (d, *J* = 8.1 Hz, 2H), 7.10 (d, *J* = 8.6 Hz, 2H), 6.96 (dt, *J* = 1.16, 7.3 Hz, 2H), 6.87-6.92 (m, 6H), 6.69 (s, 2H), 5.52 (s, 2H), 5.43 (s, 2H), 2.04 (s, 6H), 0.96 (s, 6H), -2.23 (s, 6H). ^{13}C{^{1}H} NMR (100 MHz, $CDCl_3$): *δ* 146.8, 146.4, 145.5,

143.9, 143.3, 140.7, 133.8, 129.0, 128.2, 127.3, 125.33, 125.28, 124.78, 124.6, 124.2, 123.3, 122.8, 121.7, 120.9, 110.6, 80.9, 54.3, 51.7, 39.7, 18.0, 2.6.

2. Polymerization Experiments and Polymer Characterization

2.1 Experimental procedures in the PPR platform

Propene polymerization experiments were performed in a Freeslate Parallel Pressure Reactor setup with 48 reaction cells (PPR48), fully contained in a triple MBraun glovebox operating under nitrogen. The cells, each with a liquid working volume of 5.0 mL, featured an 800 rpm magnetically coupled stirring, and individual online reading/control of temperature, pressure, monomer uptake, and monomer uptake rate. Experiments were carried out according to established experimental protocols[2–4] detailed below.

Prior to the execution of a polymerization library, the PPR modules undergo 'bake-and-purge' cycles overnight (8 h at 90-140°C with intermittent dry N_2 flow), to remove any contaminants and left-overs from previous experiments. After cooling to glovebox temperature, the module stir tops are taken off, and the 48 cells are fitted with disposable 10 mL glass inserts (pre-weighed in a Mettler-Toledo Bohdan Balance Automator) and stir paddles (Table S1). The stir tops are then set back in place, and N_2 in the reactors is replaced with propene (ambient pressure). The cells are then loaded with the appropriate amounts of solvent containing TIBA as a scavenger (Table S1 and S2).

Table S1. Stir paddles, scavenger amounts, propene pressure and solvent choice for the polymerization experiments.

Condition	**T_p = 60°C**	**T_p = 100°C**
Stir Paddles	polyether ether ketone (PEEK)	Titanium
TiBA Scavenger	10 µmol	10 µmol
Activator Ratio	2	10
$p_{propene}$	95 psi (6.6 bar)	115 psi (7.9 bar)
Solvent (cell, chaser and buffer)	toluene	mixed alkane diluent (ISOPAR-G)

The system is then thermostated at the desired polymerization temperature and brought to the desired of pressure with propene (Table S1). At this point, the catalyst injection sequence is started; aliquots of (a) a solvent 'chaser', (b) a toluene solution of catalyst (variable amount, see Table S2), (c) a toluene solution of the AB or TTB activator (variable ratio, see Table S2), and (d) a solvent 'buffer', all separated by nitrogen gaps, are uploaded into the needle and subsequently injected into the cell of destination in reverse order, thus starting the reaction. The pre-catalysts were injected into the PPR cells without pre-activation. The polymerization is left to proceed under stirring (800 rpm) at constant temperature and pressure with feed of propene on demand until the desired monomer consumption has been reached (for reaction time, see Table S2), and quenched by over-pressurizing the cell with 50 psi (3.4 bar) of dry air (preferred over other possible catalyst quenchers because in case of cell or quench line leakage oxygen is promptly detected by the dedicated glove-box sensor).

2.2 Polymer workup (PPR)

Once all cells have been quenched, the modules are cooled down to glovebox temperature and vented, the stir-tops are removed, and the glass inserts containing the reaction phases are taken out and transferred to a centrifugal evaporator (Genevac EZ-2 Plus or Martin Christ RVC 2-33 CDplus), where all volatiles are removed, and the polymers are thoroughly dried overnight under vacuum. Reaction yields are double-checked against on-line monomer conversion measurements by robotically weighing the dry polymers while still in the reaction vials, subtracting the pre-recorded tare. Polymer aliquots are then sent to the characterizations.

2.3 Polymer analytical characterizations

All polymers were characterized by means of high-temperature gel permeation chromatography (GPC) and ^{13}C NMR spectroscopy. Chain end analysis with ^{1}H NMR was run on selected samples. GPC curves were recorded with a Freeslate Rapid GPC setup, equipped with a set of two mixed-bed Agilent PLgel 10 μm columns and a Polymer Char IR4 detector using *ortho*-dichlorobenzene (with BHT added as a stabilizer, [BHT] = 0.4 mg mL^{-1}). Calibration was performed with the universal method, using 10 monodisperse polystyrene samples (M_n between 1.3 and 3700 kDa).

Quantitative spectra were recorded using a Bruker Avance III 400 spectrometer equipped with a high-temperature cryoprobe for 5 mm OD tubes, on 45 mg mL^{-1} polymer solutions in tetrachloroethane-1,2-d_2 (with BHT added as a stabilizer, [BHT] = 0.4 mg mL^{-1}). Acquisition conditions for ^{13}C NMR were: 45° pulse; acquisition time, 2.7 s; relaxation delay, 3.3 s; 1-10 K transients. Broad-band proton decoupling was achieved with a modified WALTZ16 sequence (BI_WALTZ16_32 by Bruker). Acquisition conditions for ^{1}H NMR were: 90° pulse; acquisition time, 2.0 s; relaxation delay, 10 s; 16 transients.

Table S2. Propene Polymerization Experiments (PPR).

Catalyst	*T* (°C)	*p* (psi)	Scavenger/ Activator	B/Zr ratio	Yield (mg)	Cat (nmol)	*t* (s)	R_p[a]		M_n (kDa)	Average	M_w (kDa)	Average	PDI	Average	1-σ[b]	Average	[*2,1*][c]	[*3,1*][c]	*regio*$_{tot}$[d]	Average
Hf-1	60	95	TIBA/TTB	10	32	20	484	12	25	345	385	757	785	2.2	2.0	0.15	0.14	0.07	0.02	0.09	0.08
				10	86	20	552	28		392		815		2.1		0.13		0.06	0.015	0.075	
				10	103	20	539	34		434		793		1.8		0.13		0.06	0.20	0.08	
				10	83	20	568	26		370		775		2.1		0.14		0.05	0.02	0.07	
			TIBA/AB	2	56	20	2724	4	4	379	379	978	978	2.6	2.6	0.14		0.06	0.02	0.08	
			TIBA/BHT/TTB	10	70	40	299	21	20	32	31	64	62	2.0	2.0	0.67	0.67	-	0.09	0.09	
				10	78	30	254	37		27		53		2.0		0.67		0.03	0.11	0.14	
				10	26	30	1613	2		33		70		2.1		0.67		0.03	0.11	0.14	
Hf-2	60	95	TIBA/AB	2	72	20	1466	9	3	192	210	425	496	2.2	2.4	0.11	0.10	0.14	0.08	0.22	0.24
				2	23	40	5402	0		220		553		2.5		0.10		0.15	0.09	0.24	
				2	25	40	3602	1		217		509		2.3		0.10		0.16	0.10	0.26	
	100	115	TIBA/BHT/TTB	10	33	30	413	10	68	17	16	33	31	1.9	2.0	0.69	0.75	0.04	0.24	0.28	0.28
				10	112	30	106	127		14		28		2.0		0.81		0.03	0.25	0.28	
Hf-3	60	95	TIBA/AB	2	28	60	1774	1	1	1336	1454	2886	3198	2.2	2.2	0.15	0.17	0.07	n.d.	0.07	0.07
				2	53	60	3495	1		1691		3485		2.1		0.19		0.07	n.d	0.07	
				2	67	60	3179	1		1336		3222		2.4		0.17		0.07	n.d	0.07	
	100	115	TIBA/BHT/TTB	10	68	80	438	7	5	67	59	120	117	1.8	2.0	0.30	0.30	0.04	0.125	0.165	0.17
				10	49	80	892	2		51		114		2.2		0.29		0.04	0.135	0.175	
			TIBA/TTB	10	74	20	160	83	52	56	62	114	126	2.0	2.0	0.30		0.04	0.13	0.17	
				10	28	10	467	22		67		138		2.1		0.30		0.04	0.135	0.175	
Hf-4	60	95	TIBA/BHT/TTB	10	70	20	1492	8	7	1704	1933	4269	4150	2.5	2.2	0.06	0.07	0.41	0.13	0.54	0.49
				10	46	20	1778	5		2396		4778		2.0		0.07		0.36	0.12	0.48	
				10	80	20	2184	7		1698		3402		2.0		0.08		0.39	0.11	0.50	
			TIBA/TTB	2	93	20	765	22	22	1177	1159	2889	2772	2.5	2.4	0.07		0.38	0.11	0.49	
				10	82	30	618	16	16	1140		2655		2.3		0.09		0.35	0.11	0.46	
	100	115	TIBA/TTB/BHT	10	61	30	455	16	14	113	120	207	225	1.8	1.9	0.21	0.21	0.12	0.41	0.53	0.56
				10	52	30	502	12		127		243		1.9		0.21		0.14	0.44	0.58	
	100	115	TIBA/TTB	10	20	20	2786	1	3	149	135	273	263	1.8	2.0	0.21		0.13	0.43	0.56	
				10	17	20	569	5		120		252		2.1		0.21		0.14	0.41	0.55	
Hf-5	60	95	TIBA/BHT/AB	2	50	3	1357	44	44	1454	1440	2997	3246	2.1	2.3	0.03	0.03	0.10	n.d.	0.10	0.11
					35	3	2050	20	28	1556		3531		2.3		<0.02		0.12	n.d.	0.12	
					29	3	977	36		1310		3211		2.5		0.03		0.11	n.d.	0.11	
	100	115	TIBA/BHT/AB	10	44	5	605	52	59	79	79	171	164	2.2	2.1	0.087	0.10	0.12	0.06	0.18	0.18
					45	5	501	65		78		157		2.0		0.09		0.11	0.07	0.18	
			TIBA/BHT/TTB	10	38	5	747	37	37	108	108	220	220	2.0	2.0	0.10		0.13	0.06	0.19	
			TIBA/TTB	10	25	3	820	37	44	89	90	174	179	2.0	2.0	0.10		0.12	0.06	0.18	
					38	5	883	31		103		186		1.8		0.11		0.11	0.07	0.18	
					49	5	464	76		90		183		2.0		0.085		0.14	0.06	0.20	
					30		679	32		78		173		2.2		0.10		0.11	0.06	0.17	

[a] in kg mmol$_{Zr}^{-1}$ h^{-1}, [b] Fraction of stereoirregular monomeric units in %, according to the enantiomorphic-site statistical model [c] ^{13}C NMR mole fractions of 2,1 and 3,1 monomeric units, [d] sum of 2,1 and 3,1 regioerrors

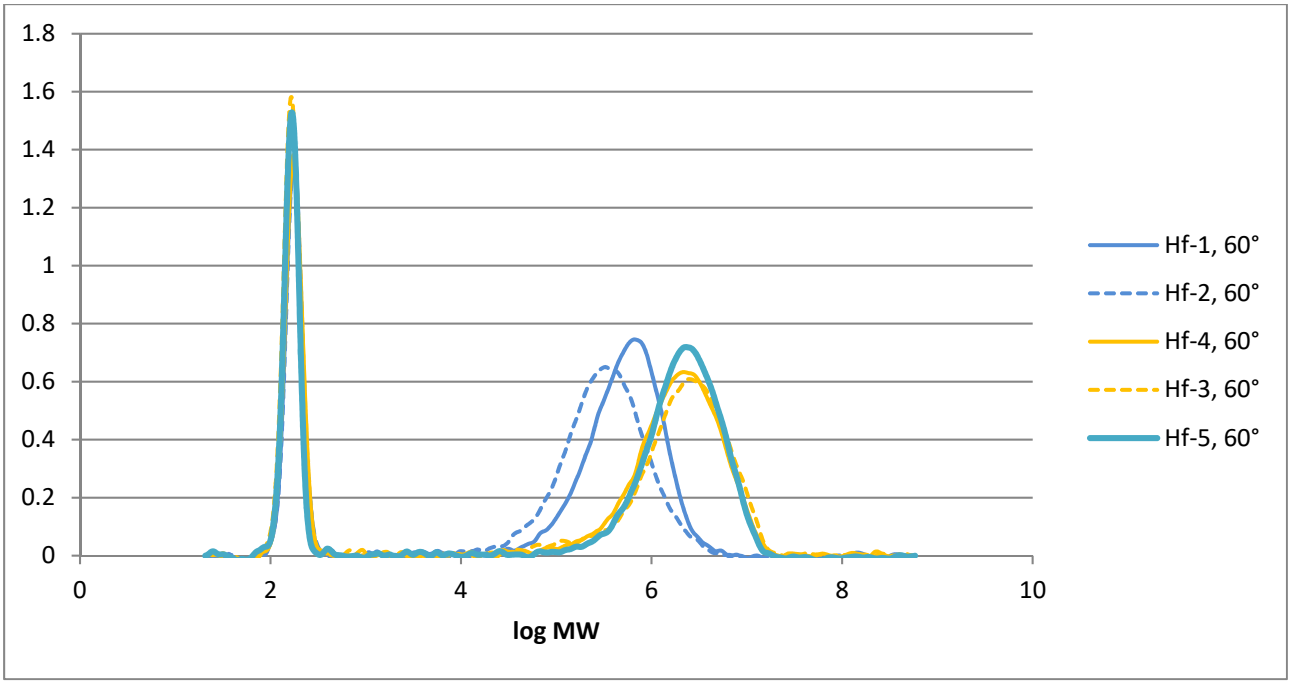

Figure S1. Exemplary Rapid-GPC curves for i-PP samples produced with catalysts Hf-1 to Hf-2 at 60°C (the sharp peak at log MW ~2 is due to the stabilizer).

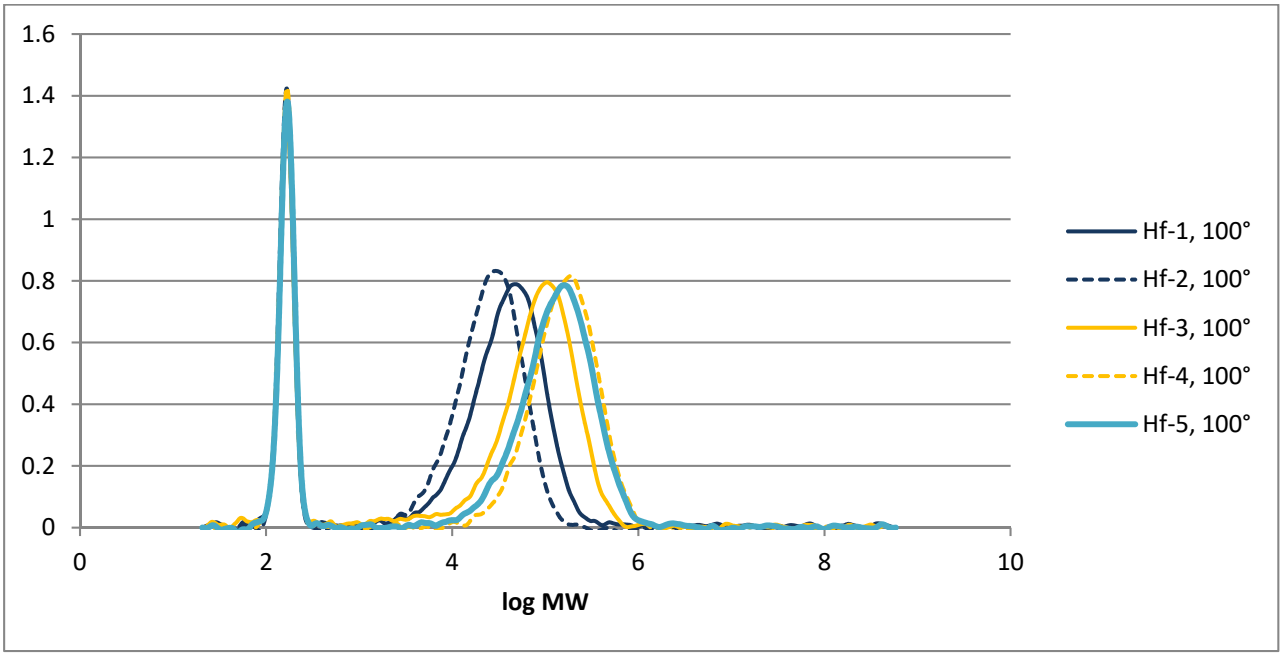

Figure S2. Exemplary Rapid-GPC curves for i-PP samples produced with catalysts Hf-1 to Hf-2 at 100°C (the sharp peak at log MW ~2 is due to the stabilizer).

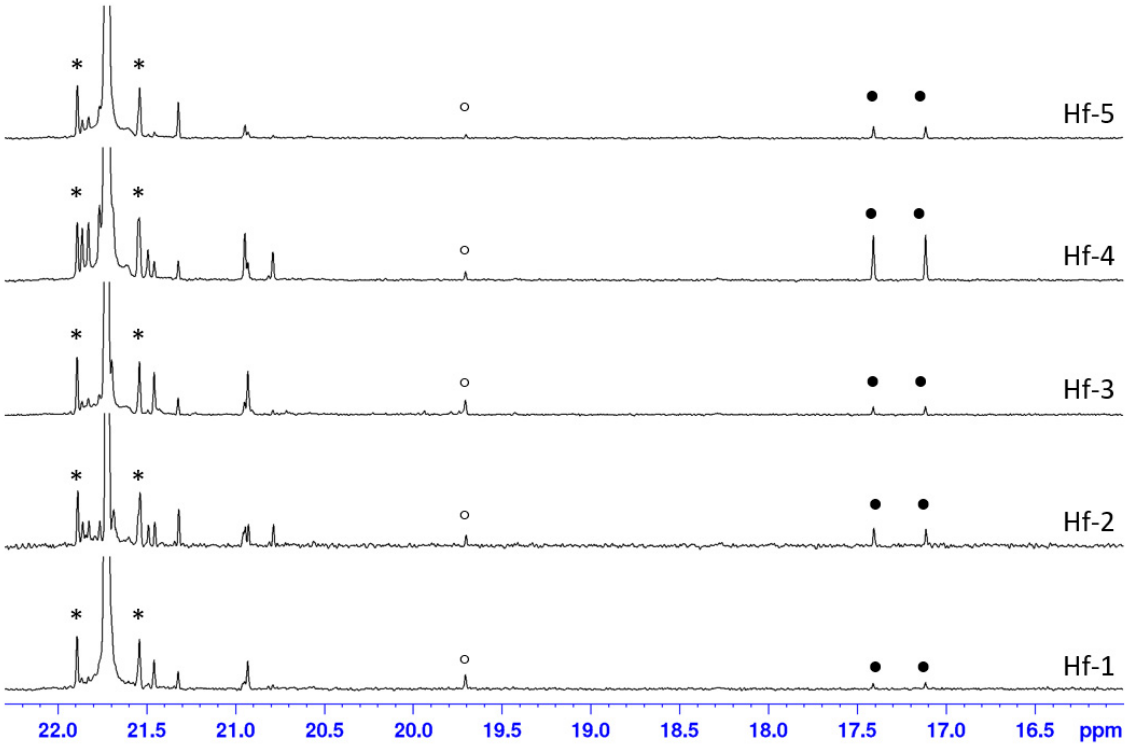

Figure S3. ^{13}C NMR spectra (expanded in the methyl region) of some representative samples obtained with catalysts Hf-1 to Hf-5 at 60°C (peaks marked with *, ◦ and • are due to satellite bands, *mmrrmm* heptad and 2,1 units, respectively).

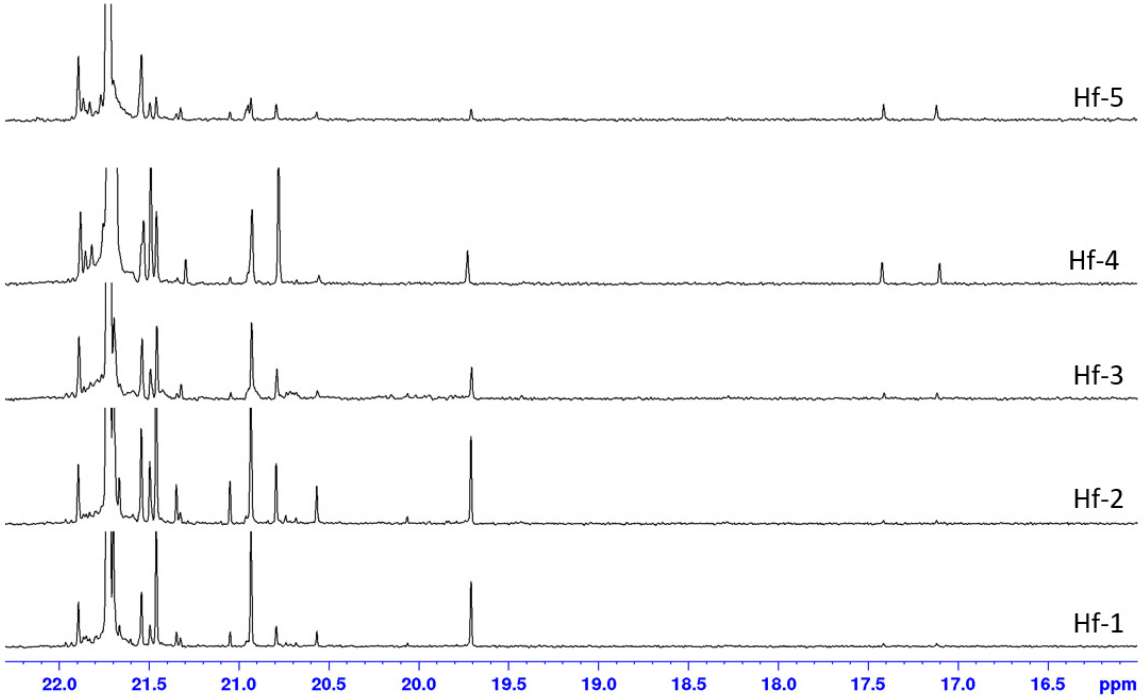

Figure S4. ^{13}C NMR spectra (expanded in the methyl region) of some representative samples obtained with catalysts Hf-1 to Hf-5 at 100°C.

3. QSAR Modeling

3.1 QSAR Modeling – Equations for Stereo-, Regioselectivity and Molecular Weight Capability Models

The following QSAR equations, previously developed for zirconocenes,[5] were used to predict the performance of catalysts **M-1** to **M-5** at

T_p = 60°C:

Stereoselectivity Model

$\Delta\Delta G^{\ddagger}_{enantio,\ exp} = 0.474\ \Delta\%V_{Bur,\ Zr} - 3.247$ (Equation S1)

Molecular Weight Model

$\Delta\Delta G^{\ddagger}_{T,\ exp} = 0.127\ \Delta\%V_{Bur,\ Zr} + 0.023\ \%V_{Bur,\ C4} + 0.039\ \%V_{Bur,\ C5\text{-}6} - 0.220\ \%V_{Bur,\ open} - 0.099\ \%V_{Bur,\ C2\text{-}3\text{-}Front} + 13.971$ (Equation S2)

Regioselectivity Model

$\Delta\Delta G^{\ddagger}_{regiotot,\ exp} = -14.267\ e^{-}_{ZrCl2,\ NPA} + 0.043\ \%V_{Bur,\ C2\text{-}3\text{-}All} + 0.031\ \%V_{Bur,\ C4} - 0.031\ \%V_{Bur,\ C5\text{-}6} - 0.529\ \%V_{Bur,\ open} + 23.619$ (Equation S3)

T_p = 100°C:

Stereoselectivity Model

$\Delta\Delta G^{\ddagger}_{enantio,\ exp} = -21.469 \times q^{-}_{ZrCl2,\ NPA} + 0.499\ \Delta\%V_{Bur,\ Zr} - 3.894$ (Equation S4)

Regioselectivity Model

$\Delta\Delta G^{\ddagger}_{regiotot,\ exp} = 0.016\ \%V_{Bur,\ C4} - 0.030\ \%V_{Bur(C5+C6)} + 0.065\ \%V_{Bur(C2+3)} - 0.682\ \%V_{Bur,\ open} -14.346\ q^{-}_{ZrCl2,\ NPA} + 26.820$ (Equation S5)

Molecular Weight Model

$\Delta\Delta G^{\ddagger}_{T,\ exp} = 0.157\ \Delta\%V_{Bur,\ Zr} + 0.030\ \%V_{Bur,\ C4} + 0.049\ \%V_{Bur(C5+C6)} - 0.178\ \%V_{Bur(C2+C3),Front} + 7.967$ (Equation S6)

The descriptor values were determined as described in Ref. 5, except for $\%V_{Bur}$ for **Hf-5**, which is used to screen steric bulk coming backwards from the active pocket. In this case, the triptycene part linked to the 5-position (going away from the active pocket) was additionally deleted.[6]

3.2 Predicted vs. observed performance for **Hf-1 to Hf-5**

Table S3. Predicted vs. observed performance in terms of stereoselectivity (Equation S1), regioselectivity (Equation S2) and molecular weight capability (Equation S3) of **Hf-1 to Hf-5** (QSAR/Experimental values) at 60°C.

Catalyst	1-σ (%)	$regio_{tot}$ (%)	M_n (kDa)
Hf-1	0.08/0.14	0.29/0.08	380/390
Hf-2	0.04/0.10	0.63/0.24	330/210
Hf-3	0.10/0.17	0.33/0.07	270/1500
Hf-4	0.03/0.07	1.32/0.50	1200/1900
Hf-5	0.01/0.03	0.19/0.11	2700/1400

Catalyst	$\Delta\Delta G^{\ddagger}_{enantio}$ (kcal/mol)	$\Delta\Delta G^{\ddagger}_{regio}$ (kcal/mol)	$\Delta\Delta G^{\ddagger}_{T}$ (kcal/mol)
Hf-1	4.8/4.4	3.9/4.8	6.0/6.1
Hf-2	5.2/4.6	3.4/4.0	5.9/5.6
Hf-3	4.6/4.2	3.8/4.8	5.8/6.9
Hf-4	5.5/4.8	2.9/3.5	6.8/7.1
Hf-5	6.2/5.4	4.1/4.5	7.3/6.9

Table S4. Predicted vs. observed performance in terms of stereoselectivity (Equation S4), regioselectivity (Equation S5) and molecular weight capability (Equation S6) of **Hf-1 to Hf-5** (QSAR/Experimental values) at 100°C.

Catalyst	1-σ (%)	$regio_{tot}$ (%)	M_n (kDa)
Hf-1	0.25/0.63	0.64/0.12	47/31
Hf-2	0.16/0.72	1.06/0.28	40/16
Hf-3	0.25/0.30	0.76/0.17	41/60
Hf-4	0.07/0.21	2.02/0.56	157/140
Hf-5	0.02/0.10	0.57/0.18	372/90

Catalyst	$\Delta\Delta G^{\ddagger}_{enantio}$ (kcal/mol)	$\Delta\Delta G^{\ddagger}_{regio}$ (kcal/mol)	$\Delta\Delta G^{\ddagger}_{T}$ (kcal/mol)
Hf-1	4.4/3.8	3.7/5.0	5.2/4.9
Hf-2	4.8/3.7	3.4/4.4	5.1/4.4
Hf-3	4.4/4.3	3.6/4.7	5.1/5.4
Hf-4	5.4/4.6	2.9/3.8	6.1/6.0
Hf-5	6.3/5.1	3.8/4.7	6.7/5.7

3.3 QSAR Models for Chain End Termination and Propensity for 1,2-to-1,3 regioerror Isomerization

3.3.1 Chain End Termination Model

Table S5. Computational descriptors, experimental performance indicator, and experimental and QSAR predicted $\Delta G^{\ddagger}_{BME\text{-}BHE_T}$ (using Hirschfeld or NPA chargers).

	Computational descriptors			Chain ends analysis			$\Delta G^{\ddagger}_{BME\text{-}BHET}$		
ID	$q^{-}_{ZrCl_2,NPA}$	$q^{-}_{ZrCl_2,HF}$	$\Delta\%V_{bur(5.0)}$	**Vinylidene**	**Ally**	**Vd/allyl**	**EXP**	**QSAR (Hirschfeld)**	**QSAR (NPA)**
Zr-1	0.408	0.0155	16.8	0.220	0.220	1.0	0.0	-0.39	0.18
Zr-2	0.414	0.0272	17.6	0.050	0.060	1.2	0.1	0.23	1.03
Zr-3	0.397	0.0074	16.2	0.062	0.013	0.2	-1.2	-0.83	-0.85
Zr-4	0.400	0.0211	17.6	0.007	0.007	1.0	0.0	0.05	0.16
Zr-5	0.396	0.0142	19.2	0.007	0.013	1.9	0.5	0.38	0.85
Hf-1	0.414	0.0594	16.9	0.020	0.105	5.3	1.2	0.95	0.61
Hf-2	0.421	0.0692	17.9	0.032	0.240	7.5	1.5	1.59	1.64
Hf-3	0.405	0.0497	16.5	0.042	0.081	1.9	0.5	0.53	-0.18
Hf-4	0.406	0.0632	18.4	0.005	0.034	6.8	1.4	1.58	1.00
Hf-5	0.400	0.0573	20.0	0.003	0.042	14.0	2.0	1.94	1.57

SUMMARY OUTPUT								
Regression Statistics								
Multiple R	0.975008							
R Square	0.950641							
Adjusted F	0.936538							
Standard E	0.233941							
Observatio	10							
ANOVA								
	df	*SS*	*MS*	*F*	*Significance F*			
Regressior	2	7.378345	3.689173	67.40902954	2.67167E-05			
Residual	7	0.383097	0.054728					
Total	9	7.761442						
	Coefficients	*andard Erro*	*t Stat*	*P-value*	*Lower 95%*	*Upper 95%*	*Lower 95.0%*	*Upper 95.0%*
Intercept	-6.53691	1.157497	-5.64745	0.000776536	-9.27395263	-3.79986296	-9.27395263	-3.79986296
X Variable	29.85651	3.444811	8.667099	5.44713E-05	21.71083209	38.00219727	21.71083209	38.00219727
X Variable	0.338334	0.066873	5.059355	0.001464409	0.180204396	0.496462788	0.180204396	0.496462788

Figure S5. Analysis of variance, chain end termination model

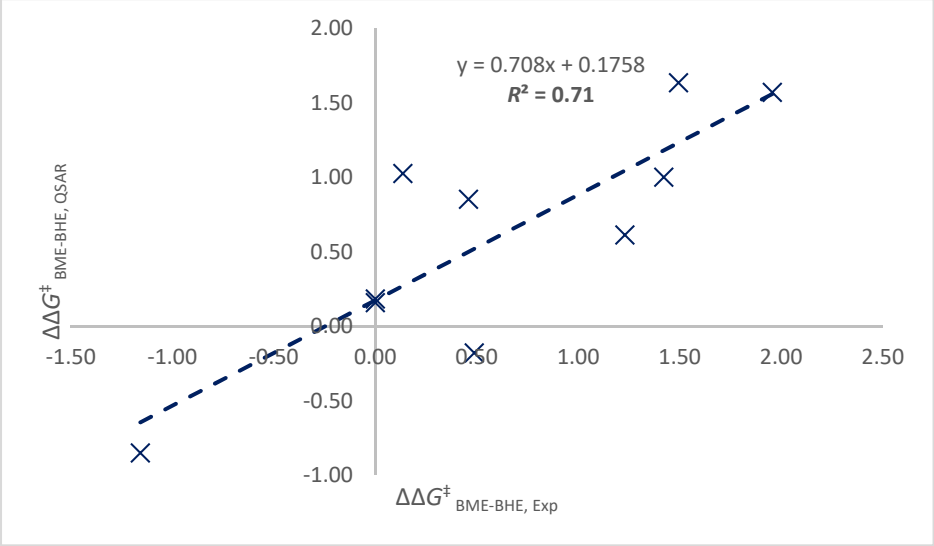

Figure S6. Correlation of experimentally observed ratio of allyl to vinyl chain ends (modeled as $\Delta\Delta G^{\ddagger}_{\text{BME-BHET, Exp}}$) at 100°C and QSAR predicted ratio ($\Delta\Delta G^{\ddagger}_{\text{BME-BHET, QSAR}}$) for catalysts **Hf-1** to **Hf-5** and **Zr-1** to **Zr-5**, using NPA rather than Hirschfeld charges.

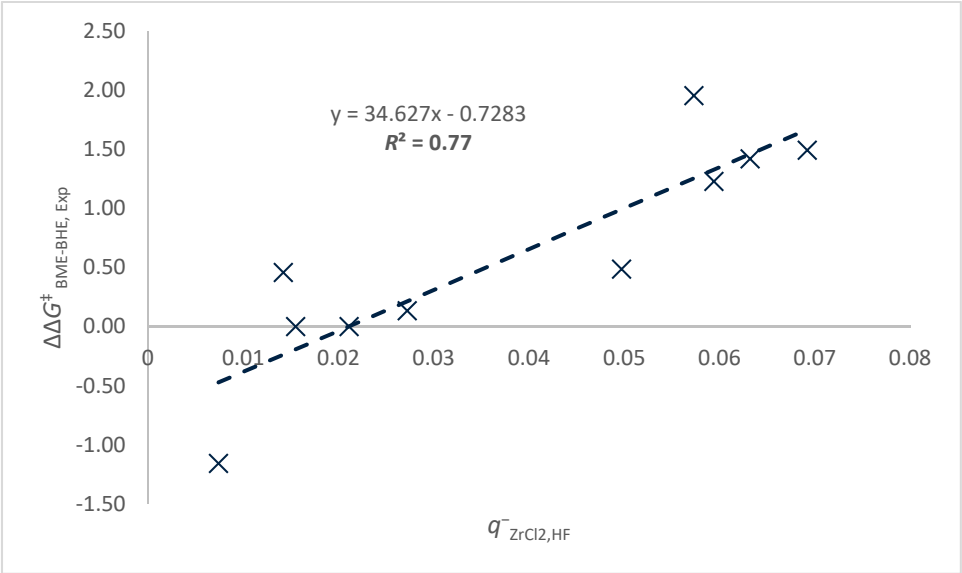

Figure S7. Single descriptor correlation of $q^{-}_{ZrCl_2,HF}$ with $\Delta G^{\ddagger}_{\text{BME-BHE}_T}$.

3.3.2 Model for Propensity for 1,2-to-1,3 regioerror Isomerization

Table S6. Computational descriptors, experimental performance indicator, and experimental and QSAR predicted $\Delta\Delta G^{\ddagger}_{1,2\text{-}2,1\text{INS-BHE}}$ (using Hirschfeld chargers).

	Computational descriptors		Regioerrors			$\Delta\Delta G^{\ddagger}_{1,2\text{-}2,1\text{INS-BHE}}$	
ID	$q^{-}_{ZrCl_2,HF}$	$\Delta\%V_{bur(5.0)}$	**2,1**	**3,1**	**2,1/3,1**	**EXP**	**QSAR**
Zr-1	0.0155	16.8	0.21	0.09	2.3	0.6	0.397
Zr-2	0.0272	17.6	0.19	0.33	0.6	-0.4	0.334
Zr-3	0.0074	16.2	0.29	0.14	2.1	0.5	0.417
Zr-4	0.0211	17.6	0.57	0.42	1.4	0.2	0.587
Zr-5	0.0142	19.2	0.33	0.02	16.5	2.1	1.716
Hf-1	0.0594	16.9	0.02	0.1	0.2	-1.2	-1.371
Hf-2	0.0692	17.9	0.04	0.25	0.2	-1.4	-1.250
Hf-3	0.0497	16.5	0.04	0.13	0.3	-0.9	-1.179
Hf-4	0.0632	18.4	0.13	0.43	0.3	-0.9	-0.737
Hf-5	0.0573	20.0	0.12	0.06	2.0	0.5	0.351

SUMMARY OUTPUT

Regression Statistics

Multiple R	0.946543431
R Square	0.895944467
Adjusted R Square	0.866214315
Standard Error	0.390222756
Observations	10

ANOVA

	df	*SS*	*MS*	*F*	*gnificance F*
Regression	2	9.177812	4.588906	30.13589	0.000363
Residual	7	1.065917	0.152274		
Total	9	10.24373			

	Coefficients	*andard Err*	*t Stat*	*P-value*	*Lower 95%*	*Upper 95%*	*Lower 95.0%*	*Upper 95.0%*
Intercept	-7.815715438	1.930754	-4.04801	0.004883	-12.3812	-3.250208013	-12.38122286	-3.250208013
X Variable 1	-41.47359499	5.746091	-7.21771	0.000175	-55.0609	-27.8862493	-55.06094069	-27.8862493
X Variable 2	0.527140359	0.111547	4.725733	0.002143	0.263374	0.790906597	0.263374121	0.790906597

Figure S8. Analysis of variance, 1,2-to-1,3 regioerror isomerization Model.

3.4 Final Energies, Enthalpies and Free Energies for species in Figure 5.

Table S7. Final energies, entropy and enthalpy corrections (T=273, 333 or 373 K, p=1.0 atm) in Hartree.

Structure	Formula	Energy(MN15/DZ)	Energy(MN15/TZ)	Num Negative	ZPE()	EnthalpyCorr (t=273, p=1.0)	EntropyCorr (t=273, p=1.0)	EnthalpyCorr (t=333, p=1.0)	EntropyCorr (t=333, p=1.0)	EnthalpyCorr (t=373, p=1.0)	EntropyCorr (t=373, p=1.0)	E	H(273)	G(273)	H(333)	G(333)	H(373)	G(373)
propene	C3H6	-117.7392684	-117.7871194	0	0.07955	0.084011159	0.026957087	0.085478331	0.034495314	0.086584344	0.039807796	-117.70757	-117.703108	-117.721169	-117.701641	-117.724753	-117.700535	-117.7272062
isobutene	C4H8	-157.0039828	-157.0669327	0	0.105299	0.111431588	0.031802029	0.113506645	0.041073986	0.11505905	0.047648562	-156.961634	-156.955501	-156.976808	-156.953426	-156.980946	-156.951874	-156.9837982
Zr																		
PP_RS_iBu_beta+	C40H43SiZr	-1884.431039	-1884.971341	0	0.709408	0.745385088	0.096752612	0.761740042	0.135996475	0.774248321	0.165551035	-1884.26193	-1884.22596	-1884.29078	-1884.2096	-1884.30072	-1884.19709	-1884.308011
PP_TS_BHE_iBu_+	C40H43SiZr	-1884.409965	-1884.94699	1	0.704801	0.740888406	0.097895568	0.757236671	0.137383324	0.769737576	0.167096702	-1884.24219	-1884.2061	-1884.27169	-1884.18975	-1884.2818	-1884.17725	-1884.289207
PP_RS_H_isobutene+	C40H43SiZr	-1884.426276	-1884.960786	0	0.705868	0.742125198	0.096952923	0.758580632	0.136351603	0.771155158	0.166018908	-1884.25492	-1884.21866	-1884.28362	-1884.20221	-1884.29356	-1884.18963	-1884.300863
PP_RS_H_isobutene_rotated+	C40H43SiZr	-1884.423495	-1884.957474	0	0.705833	0.742277129	0.097638963	0.758765621	0.137224902	0.7713609	0.167019073	-1884.25164	-1884.2152	-1884.28062	-1884.19871	-1884.29065	-1884.18611	-1884.298016
PP_TS_BHE_tBu_+	C40H43SiZr	-1884.413604	-1884.94204	1	0.705095	0.740846521	0.096513905	0.757125164	0.135621347	0.769577043	0.165071229	-1884.23695	-1884.20119	-1884.26586	-1884.18492	-1884.27578	-1884.17246	-1884.283061
PP_RS_CMe3+	C40H43SiZr	-1884.413303	-1884.952594	0	0.709214	0.745390064	0.097425168	0.76180049	0.136878361	0.774335407	0.166567109	-1884.24338	-1884.2072	-1884.27248	-1884.19079	-1884.2825	-1884.17826	-1884.289859
PP_TS_BME_iBu+	C40H43SiZr	-1884.410161	-1884.943244	1	0.707654	0.743310018	0.09605638	0.759618063	0.135095335	0.772097332	0.164510968	-1884.23559	-1884.19993	-1884.26429	-1884.18363	-1884.27414	-1884.17115	-1884.281369
PP_RS_Me_propene+	C40H43SiZr	-1884.425758	-1884.95997	0	0.705398	0.743033775	0.101025838	0.759778784	0.141639802	0.772520354	0.172119231	-1884.25457	-1884.21694	-1884.28462	-1884.20019	-1884.29509	-1884.18745	-1884.302769
Hf												E	H(273)	G(273)	H(333)	G(333)	H(373)	G(373)
PP_RS_iBu_beta+	C40H43HfSi	-1886.147723	-1886.688586	0	0.709116	0.745185688	0.097187261	0.761555814	0.136543436	0.77407268	0.166172791	-1885.97947	-1885.9434	-1886.00852	-1885.92703	-1886.01851	-1885.91451	-1886.025849
PP_TS_BHE_iBu_+	C40H43HfSi	-1886.129288	-1886.666777	1	0.704973	0.740960846	0.097275351	0.757311202	0.136629101	0.769813355	0.166253204	-1885.9618	-1885.92582	-1885.99099	-1885.90947	-1886.00101	-1885.89696	-1886.008353
PP_RS_H_isobutene+	C40H43HfSi	-1886.143205	-1886.681974	0	0.704393	0.741610315	0.100462252	0.758195755	0.140775947	0.770845934	0.17105481	-1885.97758	-1885.94036	-1886.00767	-1885.92378	-1886.0181	-1885.91113	-1886.025734
PP_RS_H_isobutene_rotated+	C40H43HfSi	-1886.142006	-1886.678244	0	0.705462	0.742092944	0.097973572	0.758618582	0.137674151	0.771234674	0.167544331	-1885.97278	-1885.93615	-1886.00179	-1885.91963	-1886.01187	-1885.90701	-1886.019264
PP_TS_BHE_tBu_+	C40H43HfSi	-1886.128342	-1886.658359	1	0.704361	0.74053797	0.098173385	0.75685948	0.137693084	0.769332759	0.167414508	-1885.954	-1885.91782	-1885.9836	-1885.9015	-1885.99375	-1885.88903	-1886.001194
PP_RS_CMe3+	C40H43HfSi	-1886.131001	-1886.67026	0	0.709316	0.74548439	0.097447722	0.761901414	0.136913155	0.774440348	0.166610335	-1885.96094	-1885.92478	-1885.99007	-1885.90836	-1886.00009	-1885.89582	-1886.007449
PP_TS_BME_iBu+	C40H43HfSi	-1886.13051	-1886.662533	1	0.707553	0.743284156	0.09640604	0.759602074	0.135532791	0.772086284	0.165006209	-1885.95498	-1885.91925	-1885.98384	-1885.90293	-1885.99374	-1885.89045	-1886.001001
PP_RS_Me_propene+	C40H43HfSi	-1886.146179	-1886.680682	0	0.706098	0.743429524	0.099518872	0.760145832	0.139769906	0.77287045	0.170006776	-1885.97458	-1885.93725	-1886.00393	-1885.92054	-1886.01418	-1885.90781	-1886.021716

Table S8. Relative enthalpies and Gibbs free energies (T=273, 333 or 373 K, p=1.0 atm) in kcal/mol.

Relative Enthalpies and Gibbs Free Energies						
H(273)	**G(273)**	**H(333)**	**G(333)**	**H(373)**	**G(373)**	**Zr**
0.0	**0.0**	0.0	**0.0**	0.0	**0.0**	PP_RS_iBu_beta+
12.5	**12.0**	12.5	**11.9**	12.4	**11.8**	PP_TS_BHE_iBu_+
4.6	**4.5**	4.6	**4.5**	4.7	**4.5**	PP_RS_H_isobutene+
6.8	**6.4**	6.8	**6.3**	6.9	**6.3**	PP_RS_H_isobutene_rotated+
15.5	**15.6**	15.5	**15.6**	15.5	**15.7**	PP_TS_BHE_tBu_+
11.8	**11.5**	11.8	**11.4**	11.8	**11.4**	PP_RS_CMe3+
16.3	**16.6**	16.3	**16.7**	16.3	**16.7**	PP_TS_BME_iBu+
5.7	**3.9**	5.9	**3.5**	6.1	**3.3**	PP_RS_Me_propene+
H(273)	**G(273)**	**H(333)**	**G(333)**	**H(373)**	**G(373)**	**Hf**
0.0	**0.0**	0.0	**0.0**	0.0	**0.0**	PP_RS_iBu_beta+
11.0	**11.0**	11.0	**11.0**	11.0	**11.0**	PP_TS_BHE_iBu_+
1.9	**0.5**	2.0	**0.3**	2.1	**0.1**	PP_RS_H_isobutene+
4.5	**4.2**	4.6	**4.2**	4.7	**4.1**	PP_RS_H_isobutene_rotated+
16.1	**15.6**	16.0	**15.5**	16.0	**15.5**	PP_TS_BHE_tBu_+
11.7	**11.6**	11.7	**11.6**	11.7	**11.5**	PP_RS_CMe3+
15.2	**15.5**	15.1	**15.5**	15.1	**15.6**	PP_TS_BME_iBu+
3.9	**2.9**	4.1	**2.7**	4.2	**2.6**	PP_RS_Me_propene+

4. References

(1) Schöbel, A.; Herdtweck, E.; Parkinson, M.; Rieger, B. Ultra-Rigid Metallocenes for Highly Iso- and Regiospecific Polymerization of Propene: The Search for the Perfect Polypropylene Helix. *Chem. - Eur. J.* **2012**, *18*, 4174–4178.

(2) Busico, V.; Cipullo, R.; Mingione, A.; Rongo, L. Accelerating the Research Approach to Ziegler-Natta Catalysts. *Ind. Eng. Chem. Res.* **2016**, *55*, 2686–2695.

(3) Busico, V.; Pellecchia, R.; Cutillo, F.; Cipullo, R. High-Throughput Screening in Olefinpolymerization Catalysis: From Serendipitous Discovery towards Rational Understanding. *Macromol. Rapid Commun.* **2009**, *30*, 1697–1708.

(4) Ehm, C.; Mingione, A.; Vittoria, A.; Zaccaria, F.; Cipullo, R.; Busico, V. High-Throughput Experimentation in Olefin Polymerization Catalysis: Facing the Challenges of Miniaturization. *Ind. Eng. Chem. Res.* **2020**, *59*, 13940–13947.

(5) Ehm, C.; Vittoria, A.; Goryunov, G. P.; Izmer, V. V; Kononovich, D. S.; Kulyabin, P. S.; Di Girolamo, R.; Budzelaar, P. H. M.; Voskoboynikov, A. Z.; Busico, V.; et al. A Systematic Study of the Temperature-Induced Performance Decline of Ansa-Metallocenes for IPP. *Macromolecules* **2020**, *53*, 9325–9336.

(6) Kulyabin, P. S.; Goryunov, G. P.; Sharikov, M. I.; Izmer, V. V.; Vittoria, A.; Budzelaar, P. H. M.; Busico, V.; Voskoboynikov, A. Z.; Ehm, C.; Cipullo, R.; et al. Ansa -Zirconocene Catalysts for Isotactic-Selective Propene Polymerization at High Temperature: A Long Story Finds a Happy Ending . *J. Am. Chem. Soc.* **2021**, *143*, 7641–7647.